Graphical Abstract

To create your abstract, type over the instructions in the template box below.
Fonts or abstract dimensions should not be changed or altered.

Synthesis, X-ray crystal structure, and solid-state blue fluorescence of dialkylbenzo[*b*]naphtho[2,1-*d*]furan-6-one-type fluorophores

Yousuke Ooyama,* Haruka Egawa,
Toshiki Mamura and Katsuhira Yoshida*
Department of Material Science, Faculty of Science, Kochi University, Akebono-cho, Kochi 780-8520, Japan
Fax: (+81) 88-844-8359
E-mail: yooyama@hiroshima-u.ac.jp; *kyoshida@cc.kochi-u.ac.jp*

Leave this area blank for abstract info.

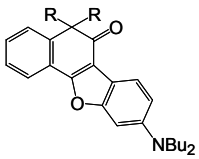

2a: R = *n*-Bu
2b: R = Octyl
2c: R = Benzyl

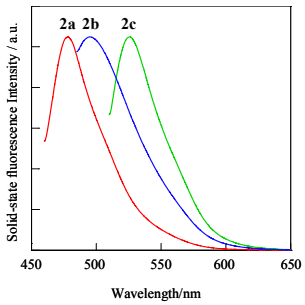

Pergamon

TETRAHEDRON

Synthesis, X-ray crystal structure, and solid-state blue fluorescence of dialkylbenzo[*b*]naphtho[2,1-*d*]furan-6-one-type fluorophores

Yousuke Ooyama,* Haruka Egawa, Toshiki Mamura, and Katsuhira Yoshida*

Department of Material Science, Faculty of Science, Kochi University, Akebono-cho, Kochi 780-8520, Japan

Abstract— Novel solid-emissive benzo[*b*]naphtho[2,1-*d*]furan-6-one-type fluorophores **2a**–**2c** constructed with a π-planar chromophore skeleton and with sterically hindered dialkyl substituents (R = butyl, octyl, and benzyl) were designed and easily synthesized. Both in cyclohexane and in the solid state, the fluorescence quantum yields (Φ) are almost the same among **2a**–**2c** ($\Phi_{solution}$ = ~ 0.5 and Φ_{solid} = ~ 0.4). Interestingly, the fluorophore **2a** exhibits strong blue fluorescence emission both in solution and in the crystalline state. To elucidate the effects of the dialkyl substituents on solid-state photophysical properties, we performed time-resolved fluorescence spectroscopic measurement, semi-empirical molecular orbital calculations (AM1 and INDO/S), and X-ray crystallographic analysis.

1. Introduction

Organic electroluminescent (EL) devices employing organic fluorophores as emitters have been the focus of considerable interest because of their possible applications as displays for mobile phones, personal computers, and televisions. Organic fluorophores exhibiting strong solid-state blue, green, and red emission are the most promising emitters for the fabrication of full-color EL devices.[1] However, organic fluorophores exhibiting strong fluorescence both in solution and in the solid state are relatively limited, because many fluorophores undergo fluorescence quenching by molecular aggregation in the solid state. In order to develop strong solid-emissive fluorophores, numerous efforts have been made on inhibiting the molecular aggregation state responsible for fluorescence quenching.[2–6] The fluorophores exhibiting strong solid-state blue emission are rare. Therefore, a new molecular design for development of strong solid-state blue emitters is required in the fabrication of clear full-color EL devices. Wong *et al*. have reported that novel ter(9,9-diarylfluorene)s with sterically hindered C9-diarylsubstituents effectively negates the steric interaction between the fluorene moieties and prevent inter-chromophore interaction, and thus, have high solid-state blue photoluminescence and electroluminescence quantum efficiencies.[2] On the other hand, Ma *et al.* recently demonstrated that strong supramolecular interactions inducing tight and rigid molecular packing without parallel stacking in crystals of cyano-substituted oligo(para-phenylene vinylene) are a key factor for the high blue luminescence efficiency of crystals.[3] In contrast, Tohnai *et al.* reported strong solid-state blue fluorescence in a tunable solid-state packing system consisting of organic salt with primary amine.[4] Generally, in order to produce fluorescent dyes exhibiting strong fluorescence in the solid state as well as in solution, the key point is to remove strong intermolecular interactions between fluorophores causing fluorescence quenching in molecular aggregation states.

Recently, we designed and synthesized novel dialkylbenzo[*b*]naphtho[2,1-*d*]furan-6-one-type fluorophores (**2a**–**2c**), which consist of a π-planar chromophore skeleton with sterically hindered dialkyl substituents.[7] The fluorophore **2a** with dibutyl groups exhibits strong blue fluorescence emission both in solution and in the crystalline state. In this study, to elucidate in

Keywords: Solid-state fluorescence; Heterocycles; Crystal structures; Dyes; Optical property.
* Corresponding author. Tel.: +81 88 844 8296; fax: +81 88 844 8359; e-mail: kyoshida@cc.kochi-u.ac.jp; yooyama@hiroshima-u.ac.jp.

detail the effects of the dialkyl substituents on solid-state photophysical properties, we performed time-resolved fluorescence spectroscopic measurement, semi-empirical molecular orbital calculations (AM1 and INDO/S), and X-ray crystallographic analysis. The relationships between the observed photophysical properties and the chemical and crystal structure of the fluorophores are discussed.

2. Results and discussion

2.1. Synthesis

The synthetic pathway is shown in Scheme 1. The starting 1,1-dialkyl-1H-naphthalen-2-ones **1a**–**1c** were prepared according to a published procedure.[8] Novel dialkylbenzo[*b*]naphtho[2,1-*d*]furan-6-one-type fluorophores **2a**–**2c** were easily obtained by the reaction of **1a**–**1c** with *m*-(dibutylamino)phenol in the presence of $FeCl_3$. However, when metal salts such as $NiCl_2$ or $CuCl_2$ were used instead of $FeCl_3$, the fluorophores **2** were not obtained. The compounds **2a** and **2c** were obtained as crystals by recrystallization from *n*-hexane, but compound **2b** was obtained in the amorphous state.

*2.2. Spectroscopic properties of fluorescent dyes **2a–2c** in solution and in the solid state*

The fluorescence spectra of **2a**–**2c** in solution and in the solid state were recorded by excitation at the wavelengths of the longest absorption maximum. The optical properties of **2a**–**2c** both in solution and in the solid state are summarized in Table 1. The absorption and fluorescence spectra of **2a**–**2c** in cyclohexane are shown in Figure 1. In cyclohexane, the absorption maxima at around 394–403 nm and the fluorescence maxima at around 439–449 nm are both red-shifted in the order of **2a** ≈ **2b** < **2c**. On the other hand, the fluorescence quantum yields (Φ) are almost the same among **2a**–**2c** (Φ = ~ 0.5). The absorption maxima of **2a**–**2c** show a small bathochromic shift of 11–12 nm from cyclohexane to acetonitrile, while the fluorescence maxima show a large bathochromic shift of 97–98 nm, so that the Stokes shift values in a polar solvent become larger than those in a non-polar solvent. Similar spectral changes are generally observed for many fluorescent dyes whose dipole moments in the excited state are larger than those in the ground state. Time-resolved fluorescence spectroscopy of **2a**–**2c** indicated that the fluorescence decays of **2a**–**2c** could be fit a monoexponential function indicating emission from the singlet excited state in all solutions. The ratio of nonradiative constant to radiative constant (k_{nr}/k_r) is close to unity in cyclohexane and 1,4-dioxane, but is 0.7–0.8 in acetonitrile. The fluorescence life time (τ_f) values of **2a**–**2c** showed solvent dependence and increased with an increase in solvent polarity: the τ_f values of **2a**–**2c** were 4.9–5.4 ns in cyclohexane, but 8.2–9.8 ns in acetonitrile.

Of particular interest are the solid-state photophysical properties. Table 2 and Figure 2 show the spectroscopic properties of **2a**–**2c** in the crystalline states. The crystals of **2a** and **2c** exhibit strong blue and green fluorescence respectively. On the other hand, **2b** was obtained not as crystals but in a solid-like amorphous state and exhibited strong bluish green fluorescence. The fluorescence quantum yields (Φ) of **2a**–**2c** were 0.40, 0.37**,** and 0.45 respectively. It is noteworthy that the Φ values of **2a** and **2c** were almost the same in cyclohexane and in the solid state. Consequently, these results also demonstrated that the solid-state photophysical properties of **2a** and **2c** are close to their photophysical properties in solution. Time-resolved fluorescence spectroscopy of **2a**–**2c** indicates that the fluorescence quantum yield depends on the ratio of radiative rate constant to nonradiative rate constant: (k_r/k_{nr}) = **2c** (0.82) > **2a** (0.66) > **2b** (0.59). However, the Φ value of **2b** in the amorphous state is smaller than that of **2b** in cyclohexane. This is presumably due to the disturbance of light scattering of the aggregates in the amorphous state.[9] Furthermore, the fluorescence life time (τ_f) values of **2a**–**2c** in the solid state were 4.2, 3.3, and 6.7 ns, respectively, which are different from those of **2a**–**2c** in cyclohexane. On the other hand, the wavelengths of the emission maximum of **2a** (λ_{em} = 478 nm), **2b** (λ_{em} = 495 nm), and **2c** (λ_{em} = 526 nm) are red-shifted by 38, 56, and 77 nm compared with that in cyclohexane, respectively. From the results of fluorescence spectra and time-resolved fluorescence spectroscopy of **2a**–**2c** both in solution and in the solid state, it was considered that the molecular arrangement and orientation in the crystalline state cause the shift of the wavelengths of the solid-state emission maximum.[4, 10, 11]

2.3. Semi-empirical MO calculations (AM1, INDO/S)

The photophysical spectra of **2a**–**2c** were analyzed by semi-empirical molecular orbital (MO) calculations. The molecular structures were optimized using the MOPAC/AM1 method[12], and the INDO/S method[13] was then used for spectroscopic calculations. The calculated absorption wavelengths and the transition character of the first absorption bands are listed in Table 3. As shown in Figure 3, the optimized geometries of **2a**–**2c** are chair-shaped because one of the alkyl groups and the 9-dibutylamino group are located on opposite sides of the molecular π-plane. The values of the dipole moment in the ground state are 3.89 for **2a**, 3.86 for **2b**, and 3.64 for **2c**, and the differences between the dipole moments ($\Delta\mu$) of the first excited state and the ground state are 8.25 for **2a**, 8.23 for **2b**, and 8.43 for **2c**. These calculations indicate that the three compounds have similar large dipole moments in the excited state, which explains well the experimental observations that compounds **2a**–**2c** showed a bathochromic shift of their fluorescence maxima in polar solvents and that the Stokes shift values for compounds **2a**–**2c** in acetonitrile are much larger than those in cyclohexane.

The calculated absorption wavelengths and the oscillator strength values are almost the same among the three compounds because of the non-conjugated linkage of the substituents (R = butyl, octyl, and benzyl) to the chromophore skeleton, although the calculated absorption wavelengths are blue-shifted. Deviation of the INDO/S calculations, giving higher transition energies compared with the experimental values, has generally been

observed.[14] The calculated oscillator strengths (*f*) of the three compounds are also almost identical, which is well compatible with the observed spectra in cyclohexane. The calculations show that the excitation bands for compounds **2a**–**2c** are mainly assigned to the transition from the highest occupied molecular orbital (HOMO) to the lowest unoccupied molecular orbital (LUMO), where HOMOs were mostly localized on the 9-dibutylaminobenzofurano moiety, and LUMOs were mostly localized on the naphthalenone moiety. The changes in the calculated electron density accompanying the first electron excitation are shown in Figure 4, and indicate a strong migration of intramolecular charge-transfer character for **2a**–**2c**.

*2.4. X-ray crystal structure of fluorescent dye **2a***

In order to investigate the effect of crystal structure on the solid-state photophysical properties, we performed X-ray crystallographic analysis of **2a**. The crystal system was an orthorhombic space group Pbca with Z = 8. The packing structure demonstrates that the molecules are arranged in a "herring-bone" fashion. As shown in Figure 5, the molecules in the crystals of **2a** are packed in a structural form shaped like a chair because one of the butyl groups and the 9-dibutylamino group are located on opposite sides of the molecular π-plane. Good correlation was observed between the bond length and bond angle of **2a** from semi-empirical MO calculation and the values obtained from the X-ray crystal structure experimentally. We expected that such a stereostructure with sterically hindered substituents (dialkyl and 9-dibutylamino groups) prevents the fluorophores from forming short intermolecular contacts responsible for fluorescence quenching in the solid state. In fact, the fluorophore **2a** has only two edge-to-edge interatomic contacts of less than 3.60 Å between neighboring fluorophores in the crystal structure. From these results, we propose a favorable stereostructure for solid-state fluorescence. For example, the H-shaped fluorophores with four bulky substituents located on both sides of the π plane, leading to inhibition of the π–π interactions between the fluorophores, would exhibit not only strong solid-state fluorescence but would also display almost the same fluorescence properties in solution and in the solid state.

3. Conclusions

Novel dialkylbenzo[*b*]naphtho[2,1-*d*]furan-6-one-type fluorophores (**2a**–**2c**) with sterically hindered dialkyl substituents were designed and conveniently synthesized, and their absorption and fluorescence properties investigated in solution and in the solid state. The fluorophore **2a** exhibits strong blue emission both in solution and in the solid state. X-ray crystal analysis of **2a** has demonstrated that the chair-shaped molecular structure with sterically hindered dialkyl substituents and the 9-dibutylamino group prevents the fluorophores from forming short intermolecular contacts and thus produces intense solid-state fluorescence emission. It was confirmed that the design of fluorophores with bulky dialkyl substituents and with non-conjugated linkage to the fluorophore skeleton can efficiently prevent the short π–π contact between fluorophores in molecular aggregation states and can exhibit strong fluorescence in the crystalline state.

4. Experimental section

4.1. General procedure

Melting points were measured with a Yanaco micro melting point apparatus MP-500D. IR spectra were recorded on a JASCO FT/IR-5300 spectrophotometer for samples in KBr pellet form. Absorption spectra were observed with a JASCO U-best30 spectrophotometer and fluorescence spectra were measured with a JASCO FP-777 spectrophotometer. Single-crystal X-ray diffraction was performed on Rigaku AFC7S diffractometer. Fluorescence lifetimes were determined with a time-resolved spectrophotometer. For the measurement of the solid-state fluorescence excitation and emission spectra of the crystals, a JASCO FP-777 spectrometer equipped with a JASCO FP-1060 attachment was used. The fluorescence quantum yields (Φ) were determined by using 9,10-bis(phenylethynyl)anthracene (Φ = 0.84, λ_{ex} = 440 nm)[15] in benzene as the standard. The solid-fluorescence quantum yields (Φ) were determined by using a calibrated integrating sphere system (λ_{ex} = 325 nm). Elemental analyses were recorded on a Perkin Elmer 2400 II CHN analyzer. ^{1}H NMR spectra were recorded on a JNM-LA-400 (400 MHz) FT NMR spectrometer with tetramethylsilane (TMS) as an internal standard. Column chromatography was performed on silica gel (KANTO CHEMICAL, 60N, spherical, neutral).

4.2. Synthesis

*4.2.1. General synthetic procedure for compounds (**2a**–**2c**) by the reaction of 1,1-dialkyl-2-naphthalenone (**1a**–**1c**) with m-(dibutylamino)phenol*

To a solution of **1** (7.81 mmol) and $FeCl_3$ (11.7 mmol) in DMSO (20 ml) was added *m*-(dibutylamino)phenol (11.7 mmol) with stirring at 110 °C. After further stirring for 11-20h, the reaction mixture was poured into water. The resulting precipitates were filtered, washed with water and dried. The precipitates were extracted with CH_2Cl_2. The organic extract was washed with water. The CH_2Cl_2 extract was evaporated and the residue was chromatographed on silica gel (CH_2Cl_2 : ethyl acetate = 10 : 1 as eluent) to give **2a**–**2c**.

*4.2.2. 5,5-Dibutyl-9-dibutylamino-5H-benzo[b]naphtho[2,1-d]furan-6-one (**2a**)*

Yield 30%. mp 134–136 °C; FTIR (KBr)/cm^{-1} 1631; ^{1}H NMR (400 MHz, $CDCl_3$) δ = 0.54–1.13 (20H, m), 1.35–1.44 (4H, m), 1.57–1.66 (4H, m), 1.74–2.34 (4H, m), 3.47 (4H, t), 6.76 (1H, dd, *J* = 2.2 and 8.56 Hz), 6.80 (1H, d, *J* = 2.2 Hz), 7.37–7.45, (4H, m), 7.92–7.96 (1H, m); ^{13}C NMR

(400 MHz, $CDCl_3$) δ = 13.7, 14.0, 20.4, 23.0, 26.4, 29.3, 43.5, 51.4, 57.8, 93.7, 110.6, 112.2, 115.4, 121.7, 122.3, 125.8, 126.4, 126.5, 129.4, 145.5, 147.8, 157.8, 161.9, 198.6. Found: C, 81.01; H, 9.28; N, 3.09. $C_{32}H_{43}NO_2$ requires: C, 81.14; H, 9.15; N, 2.96.

*4.2.3. 5,5-Dioctyl-9-dibutylamino-5H-benzo[b]naphtho[2,1-d]furan-6-one (**2b**)*

Yield 21%. FTIR (KBr)/cm^{-1} 1651; ^{1}H NMR (400 MHz, $CDCl_3$) δ = 0.78–1.29 (36H, m), 1.35–1.44 (4H, m), 1.54–1.66 (4H, m), 1.76–1.85 (2H, m), 2.25–2.32 (2H, m), 3.35 (4H, t), 6.75 (1H, dd, J = 2.2 and 8.8 Hz), 6.80 (1H, d, J = 2.2 Hz), 7.37–7.41 (1H, m), 7.44 (2H, m), 7.91–7.95 (2H, m); ^{13}C NMR (400 MHz, $CDCl_3$) δ = 14.0, 14.1, 20.4, 22.6, 24.3, 29.1, 29.2, 29.4, 29.9, 31.7, 43.7, 51.4, 57.9, 93.7, 110.6, 112.2, 115.4, 121.8, 122.4, 125.8, 126.4, 126.5, 129.4, 145.5, 147.8, 157.8, 162.0, 198.6. Found: C, 81.98; H, 10.15; N, 2.53. $C_{40}H_{59}NO_2$ requires: C, 82.00; H, 10.15; N, 2.39.

*4.2.4. 5,5-Dibenzyl-9-dibutylamino-5H-benzo[b]naphtho[2,1-d]furan-6-one (**2c**)*

Yield 36%. mp 135–137 °C; IR (KBr)/cm^{-1} 1635; ^{1}H NMR (400 MHz, $CDCl_3$) δ = 0.96 (6H, t), 1.32–1.41 (4H, m), 1.53–1.62 (4H, m), 3.27–3.32 (6H, m), 3.81 (2H, t), 6.60–6.72 (6H, m), 6.84–6.91 (6H, m), 7.31 (1H, m), 7.46 (1H, m), 7.62–7.64 (1H, dd, J = 1.44 and 7.56 Hz), 7.68–7.70 (1H, d, J = 7.56 Hz), 7.89 (1H, m) ; ^{13}C NMR (400 MHz, $CDCl_3$) δ = 14.0, 20.4, 29.3, 47.9, 51.3, 60.0, 93.4, 110.3, 112.2, 115.4, 121.9, 122.2, 125.8, 126.1, 126.9, 127.5, 128.2, 128.6, 129.5, 136.4, 142.9, 147.7, 157.5, 161.6, 196.6. Found: C, 84.44; H, 7.46; N, 2.88. $C_{38}H_{39}NO_2$ requires: C, 84.25; H, 7.26; N, 2.59.

4.3. Computational methods

All calculations were performed on FUJITSU FMV-ME4/657. Semi-empirical calculations were carried out with the WinMOPAC Ver. 3 package (Fujitsu, Chiba, Japan). Geometry calculations in the ground state were carried out using the AM1 method.[12] All geometries were completely optimized (keyword PRECISE) by the eigenvactor following routine (keyword EF). Experimental absorption spectra of **2a**–**2c** were studied with the semi-empirical method INDO/S (intermediate neglect of differential overlap/spectroscopic).[13] All INDO/S calculations were performed using single excitation full SCF/CI (self-consistent field/configuration interaction), which includes the configuration with one electron excited from any occupied orbital to any unoccupied orbital, 225 configurations were considered for the configuration interaction [keyword CI (15 15)].

4.4. X-ray crystallographic studies

The data sets were collected at 23 ± 1 ˚C on a Rigaku AFC7S four-circle diffractometer by 2θ-ω scan technique, and using graphite-monochromated Mo-Kα (λ = 0.71069 Å) radiation at 50 kV and 30 mA. In all case, the data were corrected for Lorentz and polarization effects. A correction for secondary extinction was supplied. The reflection intensities were monitored by three standard reflections for every 150 reflections. An empirical absorption correction based on azimuthal scans of several reflections was applied. All calculations were performed using the teXsan[16] crystallographic software package of Molecular Structure Corporation.

*4.4.1. Crystal structure determination of compound **2a***

Crystal of **2a** was recrystallized from *n*-hexane as light yellow prism, air stable. The one selected had approximate dimensions 0.34×0.34×0.30 mm. The transmission factors ranged from 0.97 to 1.00. The crystal structure was solved by direct methods using SIR 92.[17] The structures were expanded using Fourier techniques.[18] The non-hydrogen atoms were refined anisotropically. Some hydrogen atoms were refined isotropically, the rest were fixed geometrically and not refined. Crystal data for **2a**: $C_{32}H_{43}NO_2$, M = 473.70, orthorhombic, a = 17.964(4), b = 26.276(4), c = 12.005(3) Å, U = 5666(2) $Å^3$, T = 296.2K, space group Pbca (no.61), Z = 8, μ(Mo-K_a) = 0.34 cm^{-1}, 7177 reflections measured, 6498 unique which were used in all calculations. The final R indices were R1 = 0.073, wR (F^2) = 0.237 (all data). Crystallographic data (excluding structure factors) has been deposited with Cambridge Crystallographic Data Centre as supplementary publication number CCDC 648283. Copy of data can be obtained, free of charge, on application to CCDC, 12 Union Road, Cambridge CB2 1EZ, UK [fax: +44 0 1223 336033 or e-mail: deposit@ccdc.cam.ac.uk].

Acknowledgments

This work was partially supported by a Grant-in-Aid for Science and Research from the Ministry of Education, Science, Sport and Culture of Japan (Grant 18350100) and by a Special Research Grant for Green Science from Kochi University.

References

1. (a) Tang, C. W.; VansSlyke, S. A. *Appl. Phys. Lett.* **1987**, *51*, 913; (b) Tang, C. W.; VansSlyke, S. A.; Chen, C. H. *J. Appl. Phys.* **1989**, *65*, 3610; (c) Schi, J.; Tang, C. W. *Appl. Phys. Lett.* **1997**, *70*, 1665; (d) Kraft, A.; Grimsdale, A. C.; Holmes, A. B. *Angew. Chem. Int. Ed.* **1998**, *37*, 402; (e) Mitschke, U.; Bäuerle, P. *J. Mater. Chem.* **2000**, *10*, 1471; (f) Tonzola, C. J.; Alam, M. M.; Kaminsky, W. K.; Jenekhe, S. A. *J. Am. Chem. Soc.* **2003**, *125*, 13548; (g) Yeh, H.-C.; Chan, L.-H.; Wu, W.-C.; Chen, C.-T. *J. Mater. Chem.* **2004**, *14*, 1293; (h) Chen, C.-T. *Chem. Mater.* **2004**, *16*, 4389; (i) Chiang, C.-L.; Wu, M.-F.; Dai, D.-C.; Wen, Y.-S.; Wang, J.-K.; Chen, C.-T. *Adv. Funct. Mater.* **2005**, *15*, 231; (j) Berner, D.; Klein, C.; Nazeeruddin, M. D.; de Angelis, F.; Castellani, M.; Bugnon, P.; Scopelliti, R.; Zuppiroli, L.; Graetzel, M. *J. Mater. Chem.* **2006**, *16*, 4468.
2. Wong, K.-C.; Chien, Y.-Y.; Chen, R.-T.; Wang, C.-F.; Liu, Y.-T.; Chiang, H.-H.; Hsieh, P.-Y.; Wu, C.-C.; Chou, C. H.;

Su, Y. O.; Lee, G.-H.; Peng, S.-M. *J. Am. Chem. Soc.* **2002**, *124*, 11576.
3. Li, Y.; Li, F.; Zhang, H.; Xie, Z.; Xie, W.; Xu, H.; Li, B.; Shen, F.; Ye, L.; Hanif, M.; Ma, D.; Ma, Y. *Chem. Commun.* **2007**, 231.
4. Mizobe, Y.; Tohnai, N.; Miyata, M.; Hasegawa, Y. *Chem. Commun.* **2005**, 1839.
5. (a) Fei, Z.; Kocher, N.; Mohrschladt, C. J.; Ihmels, H.; Stalke, D. *Angew. Chem. Int. Ed.* **2003**, *42*, 783. (b) Scott, J. L.; Yamada, T.; Tanaka, K. *New J. Chem.* **2004**, *28*, 447.
6. (a) Yoshida, K.; Ooyama, Y.; Miyazaki, H.; Watanabe, S. *J. Chem. Soc. Perkin Trans. 2* **2002**, 700. (b) Ooyama, Y.; Nakamura, T.; Yoshida, K. *New J. Chem.* **2005**, *29*, 447. (c) Ooyama, Y.; Okamoto, T.; Yamaguchi, T.; Suzuki, T.; Hayashi, A.; Yoshida, K. *Chem.- Eur. J.* **2006**, 7827. (d) Ooyama, Y.; Yoshikawa, S.; Watanabe, S.; Yoshida, K. *Org. Biomol. Chem.* **2006**, *4*, 3406. (e) Ooyama, Y.; Harima, Y. *Chem. Lett.* **2006**, *8*, 902. (f) Ooyama, Y.; Yoshikawa, S.; Watanabe, S.; Yoshida, K. *Org. Biomol. Chem.* **2007**, *4*, 1260.
7. Ooyama, Y.; Mamura, T.; Yoshida, K. *Tetrahedron Letters*, **2007**, 5791.
8. (a) Oussaid, A.; Pentek, E.; Loupy, A. *New J. Chem.* **1997**, *21*, 1339; (b) Loupy, A. *Microwaves in Organic Synthesis*, Wiley-VCH: Weinheim, 2002.
9. (a) Li, Z.; Dong, Y.; Mi, B.; Tang, Y.-H.; Häuβler, M.; Tong, H.; Dong, Y.; Lam, J.-W.-Y.; Ren, Y.; Sung, H.-Y.; Wong, K.-S.; Gao, P.; Willams, I.-D.; Kwok, H.-S.; Tang, B.-Z. *J. Phys. Chem. B* **2005**, *109*, 10061. (b) Chen, J.; Xu, B.; Yang, K.; Cao, Y.; Sung, H.-Y.; Williams, I.-D.; Tang, B.-Z. *J. Phys. Chem. B* **2005**, *109*, 17086.
10. Langhals, H.; Potrawa, T.; Nöth, H.; Linti, G. *Angew. Chem. Int. Ed. Engl.* **1989**, *28*, 478.
11. Dreuw, A.; Plötner, J.; Lorenz, L.; Wachtveitl, J.; Djanhan, J. E.; Brüning, J.; Metz, T.; Bolte, M.; Schmidt, M. U. *Angew. Chem. Int. Ed. Engl.* **2005**, *44*, 7783–7786.
12. Dewar, M. J. S.; Zoebisch, E. G.; Healy, E. F.; Stewart, J. J. P. *J. Am. Chem. Soc.* **1985**, ***107***, 3902.
13. (a) Ridley, J. E.; Zerner, M. C. *Theor. Chim. Acta* **1973**, *32*, 111. (b) Ridley, J. E.; Zerner, M. C.; *Theor. Chim. Acta* **1976**, *42*, 223. (c) Bacon, A. D.; Zerner, M. C. *Theor. Chim. Acta* **1979**, *53*, 21.
14. (a) Adachi, M.; Murata, Y.; Nakamura, S. *J. Org. Chem.* **1993**, *58*, 5238. (b) Fabian, W. M. F.; Schuppler, S.; Wolfbeis, O. S. *J. Chem. Soc., Perkin Trans. 2* **1996**, 853.
15. Heller, C. A.; Henry, R. A.; Mclaughlin, B. A.; Bills, D. E. *J. Chem. Eng. Data* **1974**, *19*, 214.
16. teXsan: Crystal Structure Analysis Package, Molecular Structure Corporation **1985** and **1992**.
17. Altomare, A.; Burla, M. C.; Camalli, M.; Cascarano, M.; Giacovazzo, C.; Guagliardi, A.; Polidori, G. *J. Appl. Cryst.* **1994**, *27*, 435.
18. DIRDIF94. Beurskens, P. T.; Admiraal, G.; Beurskens, G.; Bosman, W. P.; de Gelder, R.; Israel, R.; Smits, J. M. M., The DIRIF94 program system, Technical Report of the Crystallography Laboratory, University of Nijmegen, The Netherlands, **1994**.

Figure and Scheme captions

Scheme 1. Synthetic route of **2a**–**2c**.

Figure. 1 Absorption and fluorescence spectra of compounds **2a**–**2c** in cyclohexane.

Figure. 2 (a) Solid-state excitation and (b) emission spectra of the crystals of **2a–2c**.

Figure. 3 The optimized geometries of **2a**–**2c** by using MOPAC/AM1 method (a) a side view, and (b) a top view with the dipole moments in the grand states (black) and the difference dipole moments between the excited and the ground states (gray).

Figure. 4 Calculated electron density changes accompanying the first electronic excitation of **2a**–**2c**. The black and white lobes signify degreases and increase in electron density accompanying the electronic transition. Their areas indicate the magnitude of the electron density change.

Figure. 5 Crystal packing of **2a** (a) ORTEP diagram, (b) a view of the molecular packing structure, (c) a side view, and (d) a top view of the pairs of fluorophores.

Table 1 Optical properties of **2a**–**2c** in solution

	Solvent	λ_{max}^{abs}/nm[a] (ε_{max} /dm^{3}mol^{-1}cm^{-1})	λ_{max}^{fl}/nm[b]	Φ_f[c]	τ_f[d] (ns^{-1})	k_r[e] (ns^{-1})	k_{nr}[f] (ns^{-1})
2a	cyclohexane	394 (16100)	440	0.48	4.9	0.098	0.106
	1,4-dioxane	403 (15000)	489	0.53	6.8	0.078	0.069
	acetonitrile	406 (12,000)	538	0.60	8.2	0.073	0.049
2b	cyclohexane	394 (15200)	439	0.50	4.9	0.102	0.102
	1,4-dioxane	402 (15000)	488	0.52	6.8	0.076	0.071
	acetonitrile	406 (10,700)	537	0.57	8.6	0.066	0.050
2c	cyclohexane	403 (15100)	449	0.48	5.4	0.089	0.096
	1,4-dioxane	410 (15500)	496	0.50	8.1	0.062	0.062
	acetonitrile	414 (11,400)	546	0.55	9.8	0.056	0.046

[a] 2.5×10^{-5} M. [b] 2.5×10^{-6} M. [c] Φ_f values were determined using 9,10-bis(phenylethynyl)anthracene (Φ_f = 0.84, λ_{ex} = 440 nm) in benzene as a standard. [d] Fluorescence life time. [e] Radiative rate constant ($k_r = \Phi_f/\tau_f$). [f] Nonradiative rate constant ($k_{nr} = (1-\Phi_f)/\tau_f$).

Table 2 Optical properties of **2a**–**2c** in the crystalline state

	λ_{max}^{ex}/nm	λ_{max}^{fl}/nm	Φ_f[a]	τ_f[b] (ns)	k_r[c] (ns^{-1})	k_{nr}[d] (ns^{-1})
2a	446	478	0.40	4.2	0.095	0.143
2b[e]	444	495	0.37	3.3	0.112	0.191
2c	494	526	0.45	6.7	0.067	0.082

[a] The solid-fluorescence quantum yields (Φ_f) were determined by using a calibrated integrating sphere system (λ_{ex} = 325 nm). [b] Fluorescence life time. [c] Radiative rate constant ($k_r = \Phi_f/\tau_f$). [d] Nonradiative rate constant ($k_{nr} = (1-\Phi_f)/\tau_f$). [e] Amorphous.

Table 3 Calculated absorption spectra for the compounds **2a–2c**

		Absorption (calc.)			
Quinol	μ / D[a]	λ_{max} / nm	f[b]	CI component[c]	$\Delta\mu$ / D[d]
2a	3.89	379	0.68	HOMO→LUMO (92%)	8.25
2b	3.86	378	0.68	HOMO→LUMO (92%)	8.23
2c	3.64	377	0.59	HOMO→LUMO (91%)	8.43

[a]The values of the dipole moment in the ground state. [b]Oscillator strength. [c]The transition is shown by an arrow from one orbital to another, followed by its percentage CI (configuration interaction) component. [d]The values of the difference in the dipole moment between the excited and the ground states.

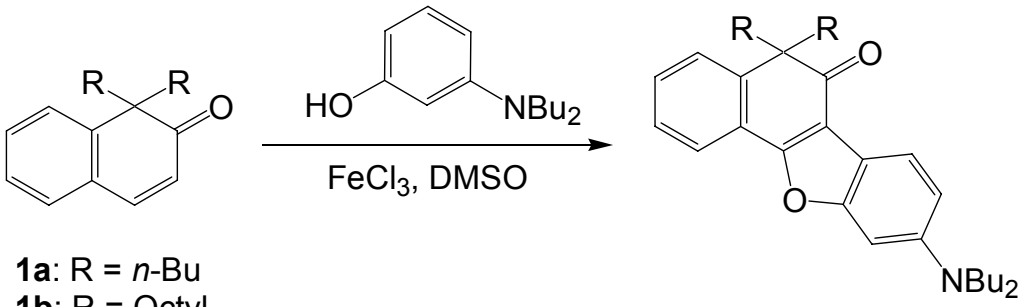

1a: R = *n*-Bu
1b: R = Octyl
1c: R = Benzyl

2a: R = *n*-Bu 30%
2b: R = Octyl 21%
2c: R = Benzyl 36%

Scheme 1 Ooyama et al.

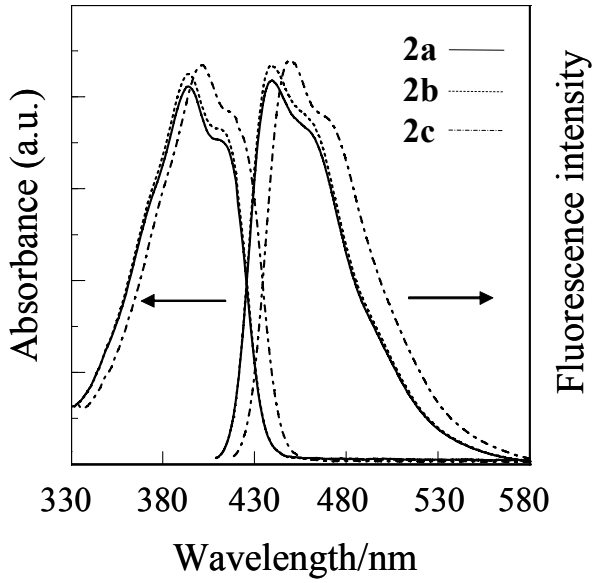

Figure. 1 Ooyama et al.

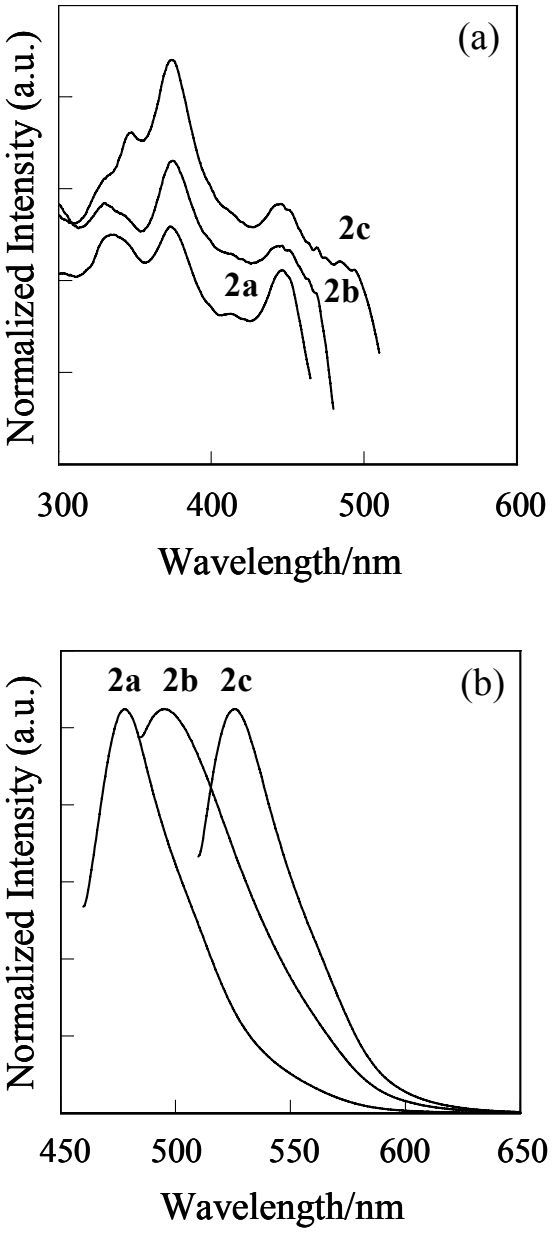

Figure. 2 Ooyama et al.

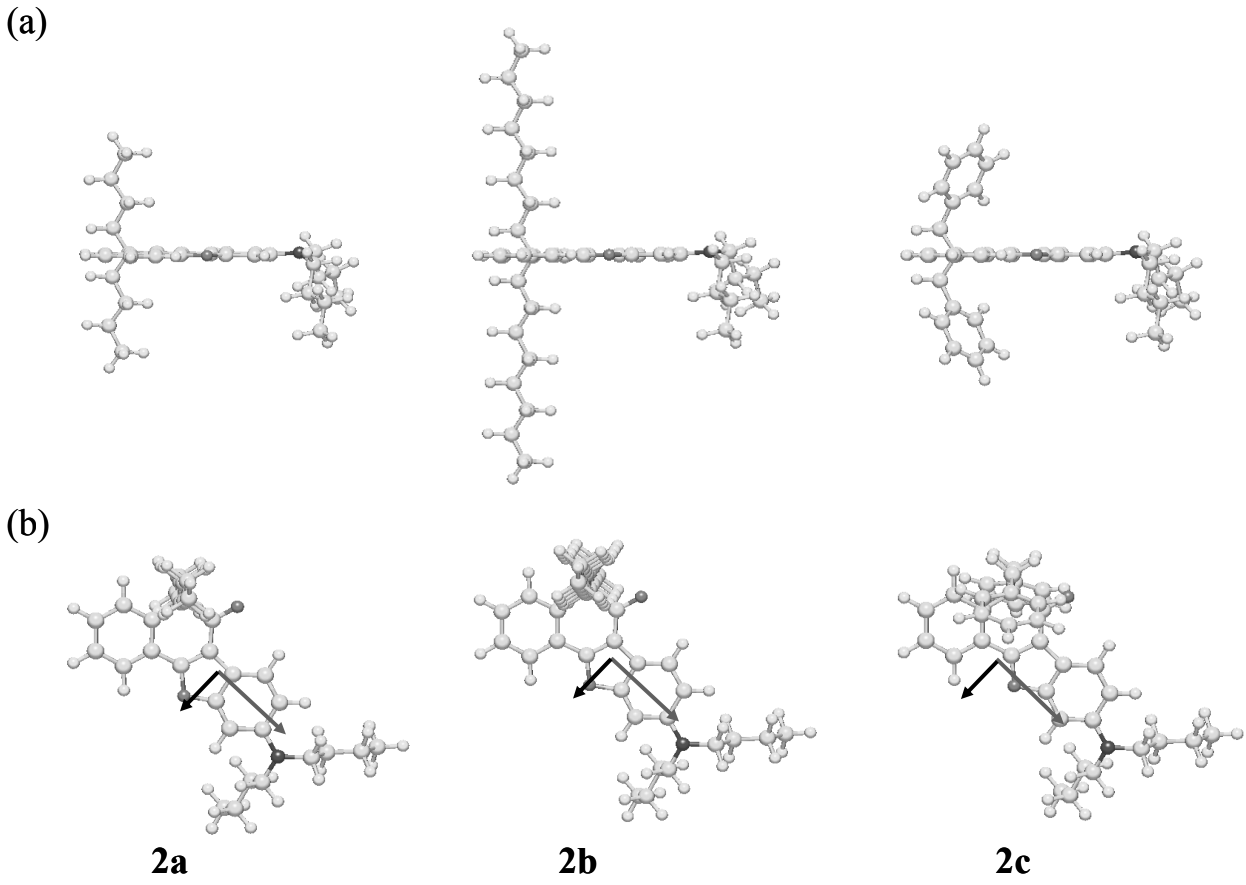

Figure. 3 Ooyama et al.

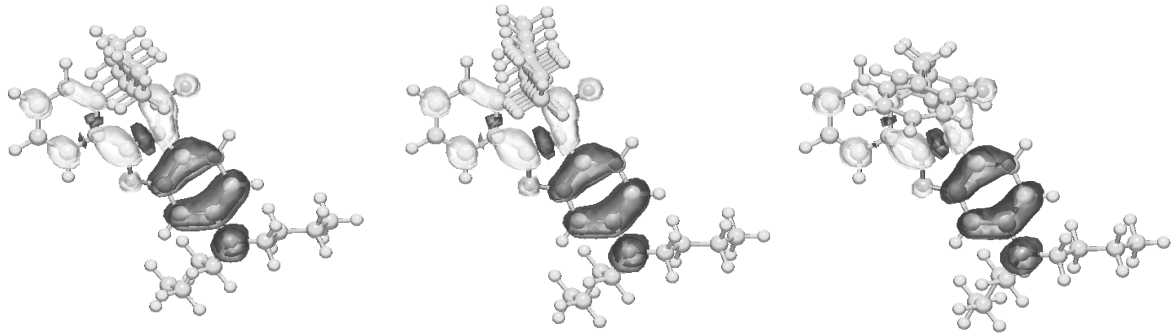

2a **2b** **2c**

Figure. 4 Ooyama et al.

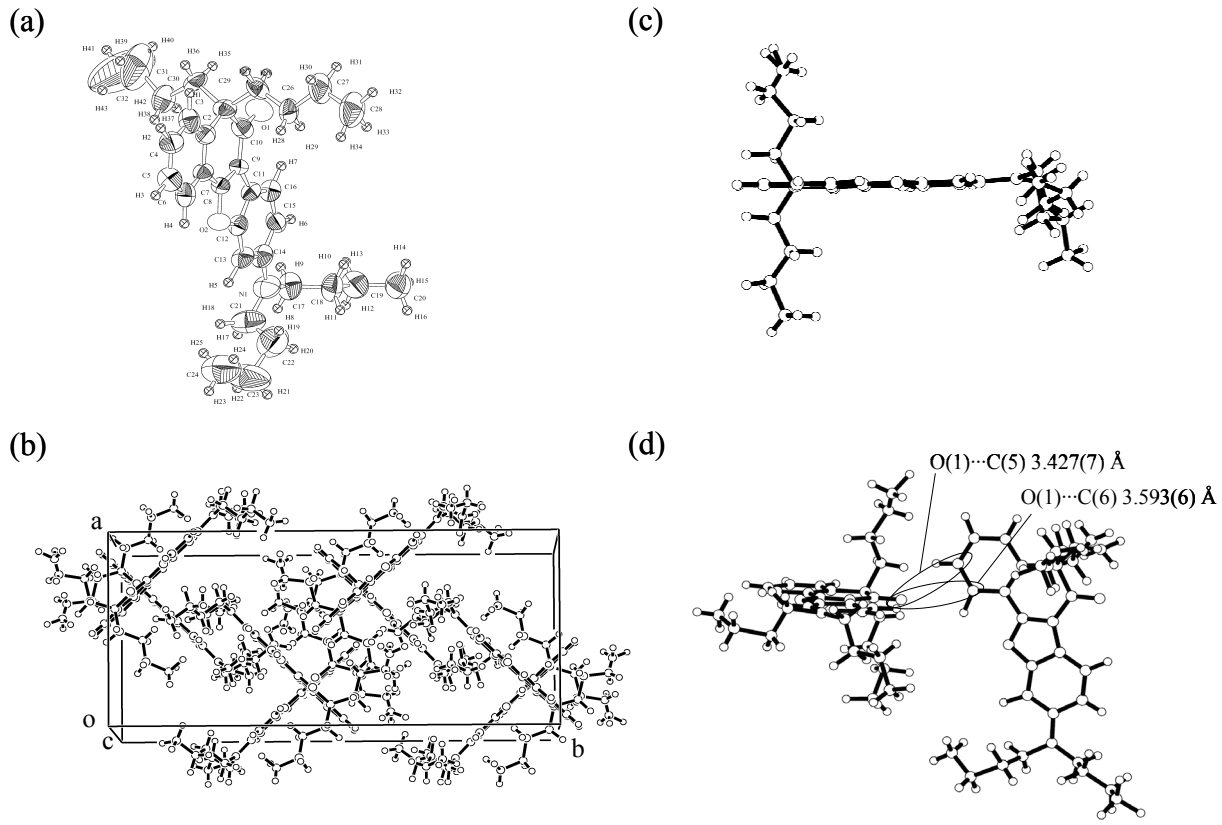

Figure. 5 Ooyama et al.